RESEARCH ARTICLE

Physico-chemical properties of waste derived biochar from community scale faecal sludge treatment plants [version 1; peer review: awaiting peer review]

Hannah Larissa Nicholas [1], Ian Mabbett [1], Henry Apsey [1], Iain Robertson [2]

[1]Department of Chemistry, Faculty of Science and Engineering, Swansea University, Swansea, Wales, SA2 8PP, UK
[2]Department of Geography, Faculty of Science and Engineering, Swansea University, Swansea, Wales, SA2 8PP, UK

v1 **First published:** 04 Aug 2022, **6**:96
https://doi.org/10.12688/gatesopenres.13727.1
Latest published: 04 Aug 2022, **6**:96
https://doi.org/10.12688/gatesopenres.13727.1

Abstract

Background: The dumping of untreated faecal sludge from non-sewered onsite sanitation facilities causes environmental pollution and exacerbates poor public health outcomes across developing nations. Long-term mechanisms to treat faecal sludge generated from these facilities are needed to resolve the global sanitation crisis and realize the Sustainable Development Goal (SDG) 6 “ensure availability and sustainable management of water and sanitation for all” by 2030. Pyrolysis of faecal sludge removes pathogens and generates biochar, which can be used as a soil enhancer.
Methods: The properties of faecal sludge biochars from three full-scale treatment plants in India were determined via Fourier transform infrared (FTIR) spectroscopy, scanning electron microscopy (SEM), energy dispersive x-ray (EDX) spectroscopy, crystal x-ray diffraction (XRD), proximate analyses, and BET surface area porosimetry.
Results: Results showed that all three biochars had low specific surface area, high alkaline pH values, high ash content, and negative surface charge. Fourier transform infrared spectra showed the same surface functional groups present in each biochar. X-ray diffraction analysis showed the mineral composition of each biochar differed slightly. Scanning electron microscopy analysis indicated a porous structure of each biochar with ash particles evident.
Conclusions: Slight differences in the ash content, surface area, pH and mineral content was observed between the three biochars.

Keywords

Biochar, Faecal Sludge, Fecal, Characterization, Properties, Pyrolysis, Sanitation

Open Peer Review

Approval Status *AWAITING PEER REVIEW*

Any reports and responses or comments on the article can be found at the end of the article.

This article is included in the Water, Sanitation & Hygiene gateway.

Corresponding author: Hannah Larissa Nicholas (hlarissa.nicholas@gmail.com)

Author roles: Nicholas HL: Conceptualization, Investigation, Methodology, Writing – Original Draft Preparation; **Mabbett I**: Conceptualization, Funding Acquisition, Methodology, Supervision, Writing – Review & Editing; **Apsey H**: Investigation; **Robertson I**: Writing – Review & Editing

Competing interests: No competing interests were disclosed.

Grant information: This work was supported by the Bill & Melinda Gates Foundation [OPP1149054], and under the grant conditions of the Foundation, a Creative Commons Attribution 4.0 Generic License has already been assigned to the Author Accepted Manuscript version that might arise from this submission. The work was also supported by Swansea University's 'SUNRISE' project funded through GCRF via EPSRC [EP/P032591/1].
The funders had no role in study design, data collection and analysis, decision to publish, or preparation of the manuscript.

How to cite this article: Nicholas HL, Mabbett I, Apsey H and Robertson I. **Physico-chemical properties of waste derived biochar from community scale faecal sludge treatment plants [version 1; peer review: awaiting peer review]** Gates Open Research 2022, **6**:96 https://doi.org/10.12688/gatesopenres.13727.1

First published: 04 Aug 2022, **6**:96 https://doi.org/10.12688/gatesopenres.13727.1

Article highlights

- The physico-chemical properties of faecal sludge biochars from full-scale pyrolysis facilities were evaluated
- Biochars recorded very alkaline pH values, high ash content, low carbon content, low specific surface area
- Similar FTIR spectra indicated the same functional organic groups present on the biochars surface
- There were differences in ash content, pH and mineral content between the biochars

Introduction

Improving sanitation along with hygiene practices and access to safe water are essential for improving socioeconomic development and health globally. Inadequate sanitation facilities and lack of clean water are key factors in the contraction of diarrhoeal diseases world-wide leading to 1.6–2.5 million deaths every year (Kosek *et al.*, 2003).

In 2000 the international community set out eight Millennium Development Goals, a template aimed at tackling the needs of the world's most poverty stricken and underprivileged (Hutton & Bartram, 2008). Target 7C of the Environmental Sustainability Goal was to reduce by half the proportion of citizens "without sustainable access to safe drinking water and basic sanitation". Since 2000, however, the proportion of the population in low and middle- income nations that use "unimproved" sanitation facilities has increased (WHO & UNICEF, 2017).

In 2015 the international community set out 17 new Sustainable Development Goals including Goal 6, to "ensure availability and sustainable management of water and sanitation for all" (UN, 2015). It is estimated that 3.6 billion people in the world still do not have access to safely managed sanitation facilities (UNICEF/WHO, 2021). Approximately 2.1 – 2.6 billion of these depend on onsite sanitation facilities (UNICEF & WHO, 2017) that generate vast quantities of untreated faecal sludge each day. In developing countries, faecal sludge (FS) collected from onsite sanitation facilities has been poorly managed, which has led to negative public and environmental health outcomes from eutrophication of surface water bodies, and contamination of groundwater and soils (Gwenzi & Munondo, 2008), and poor social and economic development (Haller *et al.*, 2007; Mara *et al.*, 2010). Long term and more sustainable solutions to deal with faecal sludge that don't involve expensive, water intensive and energy intensive sewer systems are needed.

Recent research has focused upon thermochemical treatment, with an emphasis on pyrolysis as a safe method of disposing of faecal sludge (Krueger *et al.*, 2020). Pyrolysis is the heating of biomass to temperatures of 350°C – 1000°C in an oxygen-free environment (European Biochar Foundation, 2016) which eliminates harmful pathogenic organisms within the sludge. Carbon-rich biochar produced from pyrolysis does not readily burn like charcoal (Crombie *et al.*, 2013), is safe to handle, and has been demonstrated to be an important soil amendment (Chan *et al.*, 2007). The original feedstock source, pyrolysis temperature, hold time, and heating rate are the main factors determining the characteristics of biochars (Chen *et al.*, 2008; Crombie *et al.*, 2015; Lehmann & Joseph, 2012; Tomczyk *et al.*, 2020; Weber & Quicker, 2018).

The theory behind the utilization of biochar to improve soil fertility and increase crop yield originated from observations made on the Amazonian Black Earth (*Terra Preta*). *Terra Preta* is a specific type of very dark, fertile soil discovered in the Amazon basin, containing higher nutrient levels and higher organic carbon content than the surrounding soils which are generally low in fertility (Glaser *et al.*, 2001).

There are multiple benefits to adding biochar to soil aside from improving carbon content and nutrient levels. Surface functional groups on the surface of biochar can lead to an increase in the cation exchange capacity of the soil (CEC) (Glaser *et al.*, 2001); the microporous structure of biochar can increase the water holding capacity of the soil (Gaskin *et al.*, 2007), and alkaline biochars can increase pH levels in acidic soil (Novak *et al.*, 2009). There is a considerable amount of research investigating characteristics of sewage sludge-derived biochar but less on faecal sludge biochar (Gold *et al.*, 2018). Most of the research into faecal sludge-derived biochar has focused on characterization of small-scale laboratory-produced biochar (Bleuler *et al.*, 2021; Gold *et al.*, 2018; Liu *et al.*, 2014; Woldetsadik *et al.*, 2018) while data from full-scale operations are very limited (Krueger *et al.*, 2020). Investigating the feasibility of resource recovery of operational up-scaled sludge treatment technologies and production of FS biochar with consistent properties is imperative to alleviate the sanitation crisis (Andriessen *et al.*, 2019; Strande *et al.*, 2014).

Krueger *et al.* (2020) investigated the physico-chemical properties of full-scale faecal sludge biochars from treatment plants in Warangal and Narsapur, India. They focused on solid fuel properties of biochar, particle size distribution and heavy metal concentration. Heavy metal concentrations were found to be within the limits for land application set out by the EU (EEC, 1986) and the International Biochar Initiative (IBI, 2015) apart from the Narsapur biochar which contained concentrations of lead over the IBI stated threshold.

The objective of this investigation was to assess the uniformity of biochar characteristics produced from three full-scale faecal sludge treatment plants in Wai, Warangal and Narsapur, India. This study focused more on physico-chemical properties that would contribute to biochars end-use as a soil amendment. The biochar properties determined were ash content, pH, carbon content, organic surface groups, surface charge, mineral content, pore volume, and specific surface area.

Methods

Biochar preparation

The faecal feedstocks for the preparation of the biochars used in this study were sourced from three different faecal sludge and septage processors in India: Narsapur in Andhra Pradesh,

Warangal in Telangana and Wai, Maharashtra. Warangal and Narsapur treatment plants currently have a capacity of 15m^3 per day, whereas the Wai treatment plant has a capacity of 70 m^3 per day. FS collected from septic tanks is delivered to each processing plant where it is stored in holding tanks for the homogenization of the sludge. Tide Technocrats Private Limited have several community scale faecal sludges and septage processors which sanitize faecal waste and dewaters the sludge (5–10% moisture content) using solar energy. Solar drying was managed on-site and expedited by spreading the sludge in a 10 mm layer. The sludge was pyrolyzed into biochar using a flame temperature operating range of 550–750°C. The biochar was stored in an airtight box and quenched in a water bath. The stages of the process at the community scale faecal sludge and septage processors are outlined in Figure 1. Three 5kg biochar samples were collected from each processor in September 2018.

Characterization of biochars

Chemical analysis. Elemental C, N, S and H abundances were determined at Environmental Geosciences, University of Vienna, Austria using an elemental analyzer (Vario MACRO, Elementar).

The elemental composition (C, H, N, S and O) and ash content of the biochars were used to calculate the molar element ratios H/C, C/N, and O/C. The amount of oxygen in the samples was calculated from the subtraction of total percentage carbon, hydrogen, nitrogen, and sulphur and ash content from 100 (Castan *et al.*, 2019).

Proximate analyses. Moisture and ash content of the three biochars were determined in triplicate by methods adapted from the literature (ASTM D 1762-84, 2011; Enders *et al.*, 2012).

Crucibles and covers were cleaned by heating at 750°C for 6 hours and then cooling to 105°C. This procedure volatilized residual material on the crucibles. The crucibles were transferred to desiccators and cooled to ambient temperature. The mass of crucibles and crucible covers were recorded to 0.1mg and masses determined for all samples. Approximately 1.0g of biochar was added into each crucible. For the moisture determination the crucibles and covers were heated at 105°C for 12 – 18 hours and then transferred to desiccators whilst hot. The covers were removed briefly in order to safely remove the crucibles and covers from the oven. After cooling to ambient temperature, the mass of crucibles, covers and sample were recorded to 0.1mg for all samples.

For ash determination the covered crucibles with 105°C dry biochar was placed in the furnace. The covers were adjusted so that they were askew to allow air flow into the crucibles, while reducing the possibility of physical losses. The samples were heated from ambient to 750°C at a rate of 2°C per minute. The furnace was programmed to hold the temperature at 750°C for 6 hours then allowed to cool down to ~130°C. Crucible lids were adjusted to sit flush when the temperature of 105°C was reached. The crucibles were then removed from the furnace before placing in desiccators and left to cool to ambient temperature. The mass of each crucible and crucible cover with sample was recorded to 0.1mg.

Chars were ground to <850µm in a pestle and mortar to enhance representativeness of the sample and sieved to >149µm as this lessens physical losses upon rapid heating (Enders & Lehmann, 2015).

pH and electrical conductivity. The pH of biochar samples was measured by suspending 5.0g (ground to <2mm) biochar in deionised water in a 1:10 ratio (Singh *et al.*, 2017). After 1 hour of shaking, suspensions were allowed to stand for 30 minutes before pH measurements were taken using a Voltcraft soil pH meter calibrated using pH 7 and pH 10 buffers. Electrical conductivity (EC) was measured on the same samples using

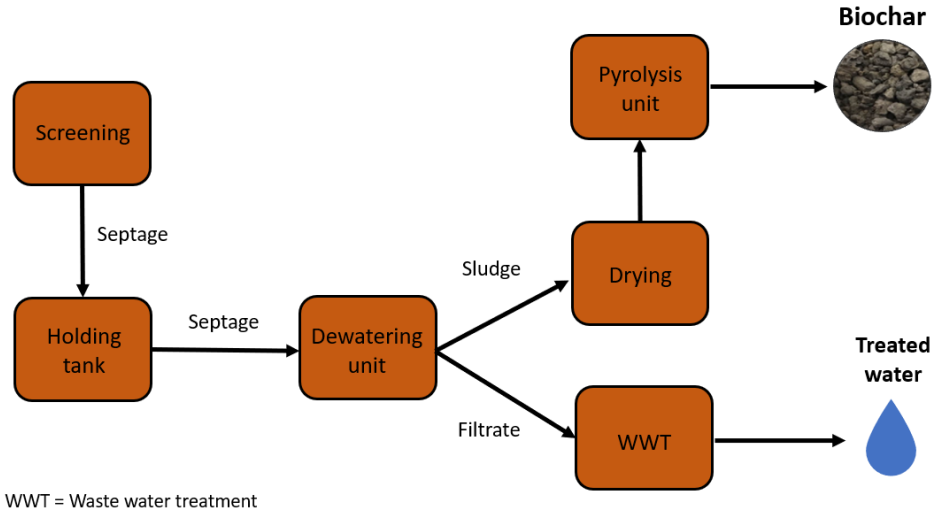

Figure 1. Flow diagram of waste through a Tide Technocrats Community Scale Faecal Sludge and Septage Processor adapted from (Tide Technocrats, n.d).

a calibrated Whatman CDM 400 EC meter. The analyses of pH and EC were performed in triplicate.

FT-IR analysis. Fourier transform infrared (FTIR) spectra were used to identify the surface organic functional groups present in the biochar. High ash content in sludge-derived biochars leads to a high mineral content with bands in the Infrared spectrum arising at similar wavenumbers to organic functional groups. To elucidate the different groups present, FTIR spectra of ashed biochars and de-ashed (acid washed) biochars were also generated.

Acid washing biochar to remove ash content (Klasson *et al.*, 2009; Lima *et al.*, 2016; Thomas Klasson *et al.*, 2014) was achieved with 0.1 M HCl at a ratio of approximately 50:1 (v/w). Samples were shaken in a Uniwist 400 at 180 rpm for 2 hours before being filtered and washed with deionised water until a pH of 7 was reached. Samples were oven-dried at 80°C overnight.

The samples were gently ground using a pestle and mortar and analyzed using a Perkin Elmer Spectrum 2 FTIR spectrophotometer applying the Attenuated Total Reflectance (ATR) method with a diamond crystal. The resulting spectra were an average of 16 scans obtained in the range from 400 to 4000 cm^{-1} with a spectral resolution of 2 cm^{-1} for biochars and 4 cm^{-1} for acid washed and ashed biochars.

Surface area. The BET (Brunauer, Emmett, and Teller) method is frequently used to determine the total surface area and pore size of materials. The BET analysis was conducted using the NOVA 2200e surface area and pore size analyzer (Quantachrome Instruments). The BET specific surface area of the three biochar samples were determined using two methods: N_2 as adsorptive gas at 77 K and CO_2 at 273 K.

Prior to these measurements, 200mg – 300mg of biochar (<2mm) were heated to 130°C under vacuum for a minimum of 4 hours. The samples were outgassed at 105 °C for a minimum of 4 hours following standard protocols. Samples were analyzed in triplicates.

For N_2 isotherms and CO_2 isotherms the BET equation was used to determine the specific surface areas from six points in the pressure region P/P_0 = 0.01–0.30 (Brunauer *et al.*, 1938). For N_2 the pore size-distributions in the pressure region P/P_0 = 0.01–0.98 were ascertained using the built-in Density Functional Theory (DFT) model assuming slit-like pores. DFT considers micropore filling process, the development of the adsorbed film thickness, and importantly capillary condensation and evaporation, thus it can model hysteresis in the adsorption/desorption mesopore region of the isotherm.

For CO_2 isotherms the pore size-distribution, the cumulative pore volume (μPV) and the cumulative surface area (μSSA) in the pressure region P/P_0 = 0.001–0.030 were determined using the built-in Grand Canonical Monte Carlo (GCMC) simulation, again, assuming pores were slit-shaped.

The benefit of using of DFT and Monte Carlo simulation methods is that they provide a combined micro-mesopore analysis.

Measurement of zeta potential. Zeta potential measurements were undertaken according to methods reported in the literature (Samsuri *et al.*, 2013; Yuan *et al.*, 2011). The zeta potential values were determined by weighing 0.045g of 63μm sieved biochar into a 250ml conical flask and adding 180 mL of 0.1M NaCl solution to each flask. Five suspensions were prepared for each biochar at pH values between 5.0 – 9.0 with the pH of each suspension adjusted using HCl . Suspensions were then dispersed ultrasonically for 30 minutes at 30 ± 1 °C in a bath-type sonicator at a frequency of 40 kHz and a power of 300 W. The samples were then left to stand for 72 hours before being measured with a Malvern Zeta Sizer Nano. In total 15 suspensions were prepared and each suspension was measured a minimum of three times.

X-ray diffraction (XRD). The X-ray diffraction (XRD) analysis of the chars was conducted on a Bruker D8 Discover XRD. This was operated at 40 kV and 40 mA and the data collected over a 2θ range of 20–70° using the Cu-Kα radiation at a scan rate of 2° min^{-1}. The main phase peaks were identified by comparing the observed XRD patterns to the standards compiled by the Crystallography Open Database (COD) (Downs & Hall-Wallace, 2003; Gražulis *et al.*, 2009; Gražulis *et al.*, 2015, Gražulis *et al.*, 2012; Merkys *et al.*, 2016; Quirós *et al.*, 2018).

SEM/EDX. SEM–EDX analysis offers detailed imaging data about the morphology and surface texture of individual particles, with characterization of the elemental composition of the analyzed volume. Scanning electron microscope (SEM) analysis was performed using a Hitachi TM3000 SEM fitted with a Bruker X-ray energy dispersive spectrometry (EDS). The two modes of operation in SEM analysis utilized here were backscattered electron imaging (BSE) and energy dispersive x-ray EDX. Biochar particles used were in the size range 150 μm– 850 μm. Prior to analysis samples were spread onto double-sided carbon tape and mounted on a SEM stub.

Cation exchange capacity. Cation exchange capacity measurements were performed in University of Santiago de Compostela, Spain, by the summation method of the exchangeable base cations of Ca, Mg, Na, K, and Al. Ammonium chloride $ClNH_4$ 1M (25ml) was added to the biochar sample (5g) and shaken manually before being left to stand overnight (16 hours). The following day, 75 ml of $ClNH_4$ 1M was added and then filtered using quantitative, low ash filter paper. (Peech *et al.*, 1947). Calcium, magnesium and aluminium were measured by PerkinElmer PinAAcle 500 Atomic Absorption Spectrometer and Na, K, were measured by Atomic Absorption Spectophotometer with an Emission Flame.

Results

Proximate analyses EC, pH and elemental analyses

All three biochars had high ash contents (Nicholas, 2022). Warangal biochar (WGL_BC) recorded the highest ash content

at 88.3% and Narsapur biochar (NSP_BC) and Wai biochar (WAI_BC) had lower ash contents at 67.0% and 62.3% respectively (Table 1.). Warangal biochar (WGL_BC) also had the lowest moisture content at 0.98% in comparison with 2.15% and 3.08% for Narsapur biochar (NSP_BC) and Wai biochar (WAI_BC) respectively. Measured pH values were high for all three biochars (11.86 – 12.45). The measured high ash content is consistent with the literature (Gold *et al.*, 2018; Koetlisi & Muchaonyerwa, 2017; Liu *et al.*, 2014). The initial feedstock of sewage sludge is high in ash and sewage sludges have been found to contain very high concentrations of Si (19–58%), Ca (5.1–7.4%), and P (3.4–4.9%) (Zielińska *et al.*, 2015). Ash content of faecal sludge is also high and has been measured at 17.0 wt.%, significantly higher than measured ash content of sawdust at 0.8% (Liu *et al.*, 2014). Increases in pH due to increases in ash content in biochars derived from sewage sludge feedstocks have been previously reported (Hossain *et al.*, 2011; Liu *et al.*, 2014). The general alkaline character of biochar likely results from the increase in quantities of alkali salts (Na, K) and salts of alkaline elements (Ca, Mg) during the pyrolysis process (Singh *et al.*, 2010).

Table 1. Proximate analyses, elemental analyses, pH, EC and surface area measurements of faecal sludge biochars.
(EC = Electrical Conductivity, C= Carbon, N= Nitrogen, S= Sulphur, Oxygen, SBET = Surface area measured by BET, TPV = Total pore volume, SSA = Specific Surface area, CEC=Cation Exchange Capacity).

Parameter	Unit	WAI BC	NSP BC	WGL BC
pH	[ ]	11.81 ± 0.01	11.82 ± 0.01	12.45 ± 0.01
EC	[mS.cm^{-1}]	2.70 ± 0.09	1.79 ± 0.17	9.00 ± 0.02
Moisture	[%]	3.08 ± 0.01	2.15 ± 0.31	0.98 ± 0.05
Ash	[%]	62.3 ± 0.32	67.0 ± 2.68	88.3 ± 0.21
C	[%]	21.11	23.79	8.06
N	[%]	1.32	1.13	0.37
H	[%]	1.55	0.73	1.15
S	[%]	0.03	0.27	0.03
O	[%]	13.69	7.08	2.09
H/C	[ ]	0.9	0.4	1.7
C/N	[ ]	18.7	24.6	25.4
O/C	[ ]	0.5	0.2	0.2
S_{BET} N_2	[m^2.g^{-1}]	3.52 ± 0.78	3.69 ± 0.36	12.07 ± 4.12
N_2 TPV	[cm^3.g^{-1}]	0.011	0.011	0.019
S_{BET} CO_2	[m^2.g^{-1}]	46.72 ± 7.0	74.20 ± 4.0	26.11 ± 2.6
CO_2 µSSA	[m^2.g-1]	63.49 ± 8.3	99.62 ± 4.5	36.76 ± 3.0
CO_2 µPV	[cm^3.g^{-1}]	0.017	0.027	0.010
CEC	[cmol.kg^{-1}]	90.0 ± 6.5	41.9 ± 2.2	129.3 ± 2.3

WGL_BC recorded the most alkaline pH value (12.25) and the largest EC value (Table 1.) which is due to the higher ash content recorded for WGL_BC (Rehrah *et al.*, 2014). There could be several reasons why the WGL biochar had a significantly higher ash content. Digestion during storage in onsite sanitation technologies can play a part in the high ash content of FS biochar (Gold *et al.*, 2018) as well as contamination of FS by sand and grit caused by poorly lined containment structures (Niwagaba *et al.*, 2014). A recent study investigating biochar from the same treatment facilities in India observed that sintered mineral depositions had to be removed from the reactor on a weekly basis (Krueger *et al.*, 2020). Therefore, it is likely that ash concentrations from biochars from these types of treatment plants will fluctuate over time.

A high ash content of biochar could be useful with regards to its end-use a soil amendment. Increased crop growth with a highly alkaline (12.1), high ash biochar treatment of acidic soil has been previously reported (Smider & Singh, 2014) The authors deemed this was a result of the release of nutrients from the ash in the biochar itself and the biochar's liming effect. It has been proposed that this liming effect is one of the main processes influencing the enhanced plant growth seen on biochar addition to soils (Jeffery *et al.*, 2011). Altering soil pH is one of several mechanisms by which biochar can improve soils and increase agricultural productivity. Therefore, highly alkaline biochars could be of benefit to acidic soils are responsible for the severe limitation of crop agriculture worldwide. Currently only a small fraction of acidic soil is used for arable crops globally but approximately 50% of the earth's potential arable lands are acidic (von Uexküll & Mutert, 1995).

The elemental composition *(Table 1.)* shows a relatively low percentage of carbon within the samples, 21–23% for NSP_BC and WAI_BC and a very low 8% for WGL_BC which is consistent with the measured ash content. Pyrolysis generally concentrates carbon in the biochar with an increase in C content relative to the feedstock frequently reported. However, most studies on sewage sludge (SS) –derived biochar show a decrease in the percentage of C in the final product relative to the feedstock (Agrafioti *et al.*, 2013; Khan *et al.*, 2013). FS- and SS–derived biochars generally have low total C concentrations in comparison with cellulose derived biochars (Tomczyk *et al.*, 2020). This is due to the high ash content in the original feedstock of faecal and sewage sludge. The measured carbon concentrations in these biochars are consistent with carbon contents reported in the literature for faecal sludge biochar 27.4– 34.9% (Gold *et al.*, 2018), 17.2 – 34.1% (Krueger *et al.*, 2020), 6.5 – 11.1% (Koetlisi & Muchaonyerwa, 2017), and 19.5% (Woldetsadik *et al.*, 2018).

Fourier transform infrared (FTIR) spectroscopy

FTIR spectra indicated that all three sludge biochars have a complex chemical bond structure with both organic matter and mineral compounds evident within the biochar. The FTIR spectra of all three biochars were similar confirming the presence of the same surface functional groups (Figure 2).

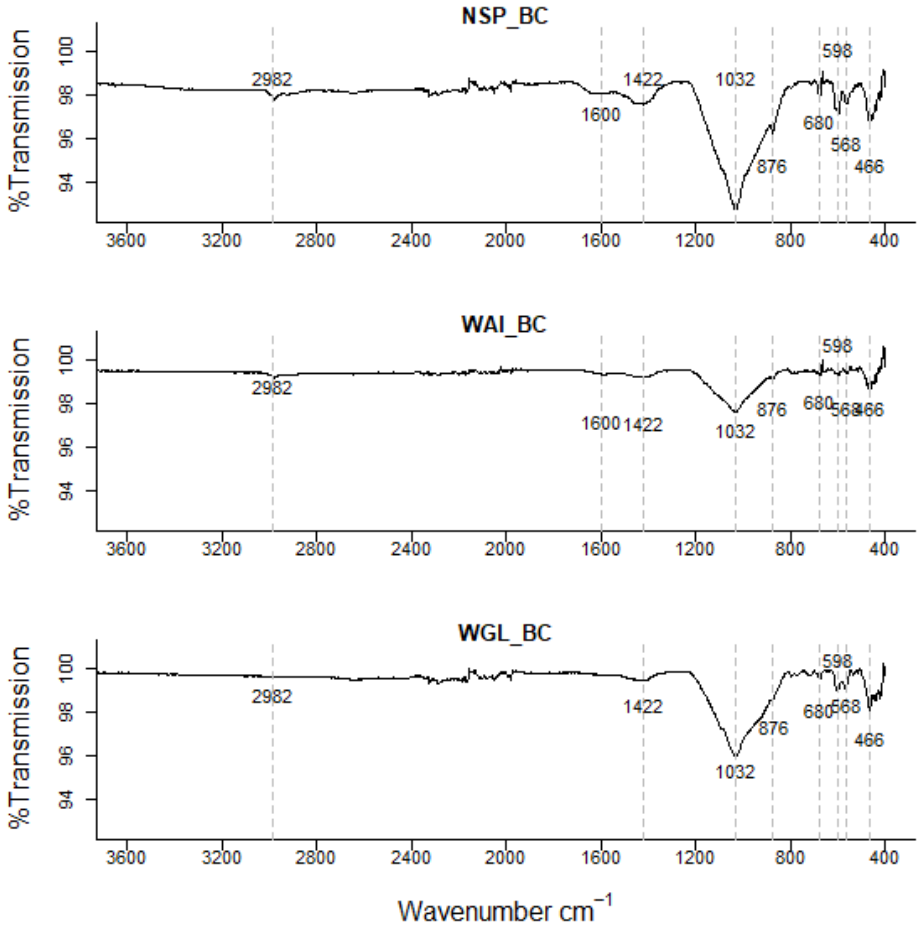

Figure 2. Fourier-transform infrared spectra (FTIR) of the three biochars NSP, WGL and WAI with dotted lines representing the main absorption (cm^{-1}) peaks.

High ash content in sludge-derived biochars leads to a high mineral content with bands arising on the spectrum at similar wavenumbers to organic functional groups. For example, a broad peak in the 1000–1200cm^{-1} region can arise due to several functional groups such as inorganic and organic silicon, phosphorus compounds, as well as C-O stretching and sulphate groups (Coates, 2004)

Low intensity peaks evident in the 3800cm^{-1} –3600cm^{-1} region relate to OH group vibrations within mineral matter (Hossain *et al.*, 2011) which indicates the presence of clay type compounds within the biochar (Table 2). Two peaks at 2980cm^{-1} and 2890cm^{-1} indicate asymmetric and symmetric aliphatic ν(CH) from terminal –CH_3 groups respectively (Socrates, 2001). However, these CH bands disappear at high temperatures due to demethylation and dehydration (Zhang *et al.*, 2015) therefore in biochar pyrolyzed at 550 – 750°C the peaks are negligible.

Small peaks in the 2700–2100 region could be due to P-OH groups in phosphorus acids and esters which produce one or two broad bands (Stuart, 2004).

A peak at 1424cm^{-1} corresponds to asymmetric stretches of carbonate groups, which correlates with the small peak at 874 cm^{-1} due to the out-of-plane bending for CO_3^{2-} (Zhao *et al.*, 2013). This could indicate the presence of calcite (calcium carbonate) in the sample. The presence of carbonate was verified as the FTIR spectrum of the acid washed biochar showed no clear peaks at 1424 cm^{-1} or 874 cm^{-1} confirming that acid washing removed carbonates from the sample (Figure 4.).

Another interesting difference between the ashed (Figure 3.) biochars and deashed biochars is a broad trough between 3400cm^{-1} and 2500 cm^{-1}. This implies the presence of O-H in carboxylic acids however there is only a very weak intensity peak at ~1700 cm^{-1} which could correspond to C=O in carboxylic acids. Other possible groups responsible for peaks within the 3400cm^{-1} and 2500 cm^{-1} region include ν(OH) from sorbed water and hydrogen bonded OH (Keiluweit *et al.*, 2010).

The low intensity peak in biochar between 1540 and 1650 could be indicative of C=O stretching vibrations for amides (Calderón *et al.*, 2006), aromatic C=C stretching and carboxylate anion vibrations (Deacon & Phillips, 1980).

Table 2. Proposed band assignments of the FTIR spectra of biochar.

Wavenumbers (cm^{-1})	Characteristic vibrations	Reference
3670 - 3650	ν(OH) from non-hydrogen bonded O-H groups	(Sharma *et al.*, 2004)
3600 - 3200	ν(OH) from sorbed water and hydrogen-bonded biochar O-H groups	(Keiluweit *et al.*, 2010)
~2980	2990-2950 cm^{-1} asymmetric aliphatic ν(CH) from terminal $–CH_3$ groups	(Socrates, 2001)
~2890	2870-2890 cm^{-1} ^{symmetric} aliphatic ν(CH) from terminal $–CH_3$ groups	(Socrates, 2001)
2700-2100	P-OH groups produce one or two broad bands in the 2700 -2100 region 2100 - 2250cm^{-1} C≡C bonds 2100 - 2360cm^{1} Silane Si-H 2100 - 2270cm^{-1} Dimides, Azides and Ketenes	(Stuart, 2004)
1700	ν(C=O) from carboxylic acids amides, esters and ketones 1740- 1650	(Socrates, 2001)
1540 - 1650	C==O stretching vibrations for amides, aromatic C=C stretching and carboxylate anion vibrations.	(Calderón *et al.*, 2006)
1580 - 1600	vibration of C=C bonds	(Davis *et al.*, 1999)
1424	Carbonate (ν_3; asymmetric stretch)	(Socrates, 2001)
1200- 950	P–O (asymmetric and symmetric stretching of $PO_2$and $P(OH)_2$ in phosphate)	(Jiang *et al.*, 2004)
1100-1000	Si-O-Si asymmetric stretching	(Falaras, 1999)
1020 - 1030	C–O stretching of ethers and primary amine C–N stretches	(Keiluweit *et al.*, 2010) (Claoston *et al.*, 2014)
~875	Out-of-plane bending for CO_3^{2-} and – ν(M-O-H) O-H bending bands from clay minerals associated with biochar	(Zhao *et al.*, 2013) (Farmer, 1974)
796 and 780	quartz doublet	(Farmer, 1974)
462-464	Si-O-Si	(Qian & Chen, 2013)
452	Si-O rocking	Abadi *et al.*, 2015

The low intensity peak in biochar between 1540 and 1650 could be indicative of C=O stretching vibrations for amides (Calderón *et al.*, 2006), aromatic C=C stretching and carboxylate anion vibrations (Deacon & Phillips, 1980).

The peak in the deashed biochar at 1580 cm^{-1} to 1600 cm^{-1} is indicative of a carboxylate ion, the conjugate base of a carboxylic acid (Deacon & Phillips, 1980; Ellerbrock & Gerke, 2021).

This peak was not evident in the ashed biochar (Figure 3.). It's been suggested that a reduction in inorganics by acid demineralization allows previously hidden carbon to emerge so increasing the amount of acidic functional groups (Lou *et al.*, 2011). In the ashed biochar there are very visible peaks ~1450cm^{-1} indicative of a carbonate stretch (CO_3^{2-}) whereas as the peaks in the acid washed samples are much less visible indicating some carbonate salts within the ash content have been successfully removed by acid demineralization.

The very broad band in the range 1200-970cm^{-1} is indicative of several functional groups. Inorganic and organic silicon and phosphorus compounds, as well as carbohydrates and sulphates can contribute to this broad peak (Wen *et al.*, 2007). Sewage chars are known to contain high phosphorus levels suggesting that the peaks observed in 1200-950cm^{-1} band arise from P containing functional groups such as asymmetric and symmetric stretching of PO_2 and $P(OH)_2$ in phosphate (Jiang *et al.*, 2004). Si-O asymmetric stretching could also be present between 1000-1100cm^{-1} (Falaras, 1999) as well as symmetric C-O stretching of ethers.

A peak at 462-464 cm^{-1} evident in both biochar and acid washed biochar is indicative of bending vibration of Si-O-Si (459-463 cm^{-1}) (Qian & Chen, 2013). In the ashed biochar this peak seems to shift to a lower wavenumber 456cm^{-1}. It is possible the signals at 462-464 cm^{-1} relate to bending vibration of Si-O-Si (459-463 cm^{-1}) and the signal at lower wavelength in the ashed biochar at 452cm^{-1} relates to Si-O rocking

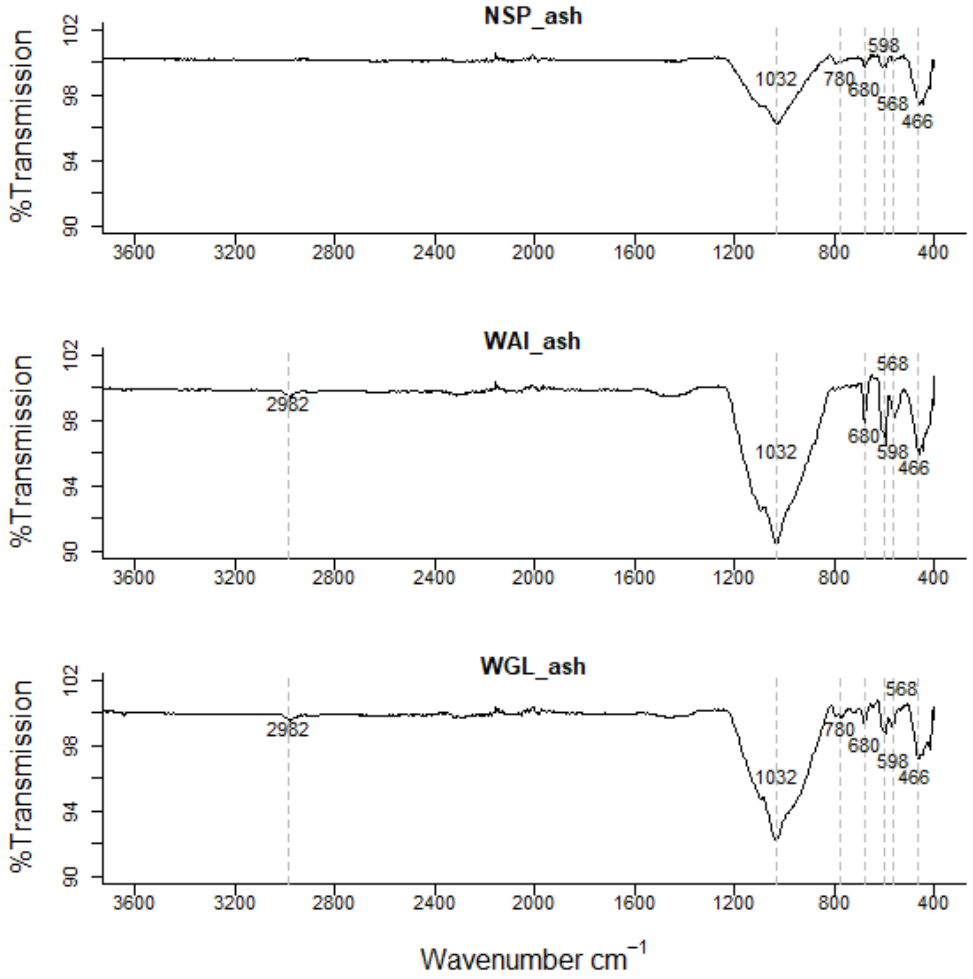

Figure 3. FTIR spectra of ashed NSP biochar, ashed WAI biochar, and ashed WGL biochar.

(Shahrokh Abadi *et al.*, 2015). A weak intensity signal at 1984 cm^{-1} is evident in the ashed biochar but not in the deashed samples. This signal could indicate metal – carbonyl bonds, typically terminal M-CO bonds occur at 2125 - 1850 cm^{-1}. A quartz doublet at 796cm^{-1} and 780cm^{-1} is evident in the ashed biochar sample (Farmer, 1974).

There are more signals recorded in the 900-400 cm^{-1} region for the ashed biochar than the deashed biochar which relate to clay minerals associated with biochar. Bands below 600 cm^{-1} can be caused by stretching inorganic compounds such as KCl and $CaCl_2$ (Hossain *et al.*, 2011).

The oxygen containing functional groups (OCFGs) present on biochars surface such as C=O groups determine its cation exchange capacity (CEC) (Banik *et al.*, 2018). It is this property that enables biochars to adsorb cationic nutrients such as NH_4^+, Ca^{2+}, K^+ within the soil and increases soils nutrient retention capability. The lack of C=O groups present in WGL_BC could affect its ability to retain nutrients and therefore its suitability as a soil amendment.

Surface area

The shape of the isotherms indicate a Type II isotherm, however, Type II isotherms are generally typified by a lack of hysteresis and no saturation at P/P_0 near to 1; typical of nonporous and macroporous adsorbents (Thommes *et al.*, 2015). A deviation from a true Type II isotherm can be described as a pseudo-type II isotherm. These isotherms are associated with delayed capillary condensation due to the small degree of pore curvature and non-rigidity of the aggregate structure of the adsorbent. (Sing & Williams, 2004).

Isotherms of each biochar indicate a degree of both mesoporosity and microporosity.

Hysteresis is present in all isotherms and can be classified as H3/H4 according to International Union of Pure and Applied Chemistry (Thommes *et al.*, 2015). Hysteresis is caused by capillary condensation and is typical of mesoporous materials. H3 and H4 loops do not tend to close until equilibrium pressure is at or close to saturation pressure. H3 type is typical for loose aggregates of plate-like particles and in porous materials

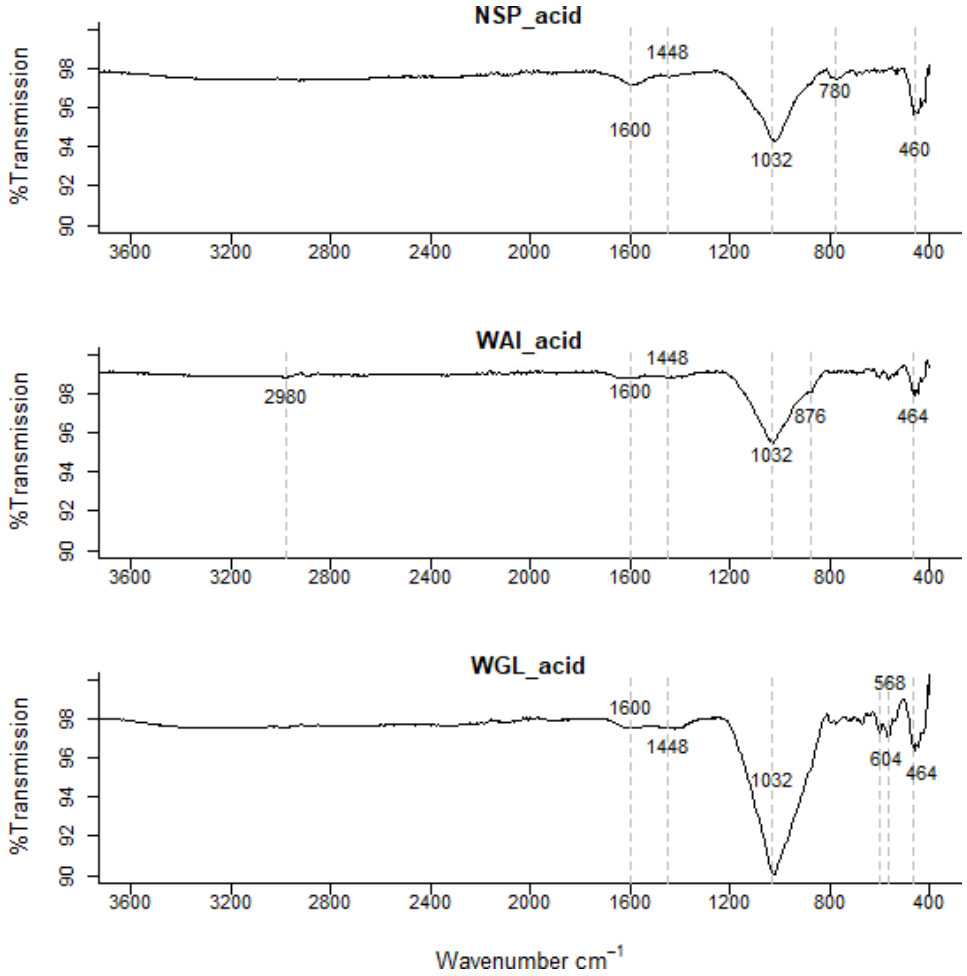

Figure 4. FTIR spectra of deashed (acid washed) NSP, WAI and WGL biochar.

typical of pore networks containing macropores not entirely filled with condensate. H4 type loops suggest presence of slit-shaped pores including pores in the micropore region and plate-like particles with spaces between the parallel plates (Mokaya & Jones, 1995) and are common with activated carbons. H4 hysteresis loops are commonly observed with more complex materials consisting of both micropores and mesopores.

Adsorption and desorption N_2 isotherms for all biochars (Figure 5.) showed low surface areas of between 3.52 – 12.07m^2g^{-1} *(Table 1)* consistent with results reported in the literature for sewage sludge biochars which have low surface areas due to high ash content (Agrafioti *et al.*, 2013; Bagreev *et al.*, 2001; Schimmelpfennig & Glaser, 2012). It has been postulated that high ash contents reduce surface area by filling or blocking access to the biochar micropores (Song & Guo, 2012).

The low nitrogen uptake of all three biochars can be characteristic of materials with small ultra-micropores that are close to the kinetic diameters of nitrogen, since molecules cannot overcome the activation energy for passing through the pores at cryogenic temperatures (Kim *et al.*, 2011). To investigate this potential microporosity further CO_2 adsorption isotherms at 273K were recorded for the three biochar samples (Figure 6).

The CO_2-based BET specific surface areas (S_{BET}, µSSA) and pore volume (µPV) values were significantly larger than the N_2-derived BET specific surface area (S_{BET}) and pore volume (TPV) values signifying that kinetic limitations with N_2 physisorption were present for all biochars and there is some degree of microporosity present.

NSP biochar showed the largest surface area measured with CO_2 and the lowest with N_2 indicating a more microporous structure whereas WGL biochar had the highest N_2 SSA and lowest CO_2 µSSA signifying a slightly less microporous and more mesoporous structure. The greatest pore size distribution at pore diameters 4–15Å was recorded for NSP biochar also indicating it had more of a microporous structure than WGL biochar which recorded relatively sparse pore size

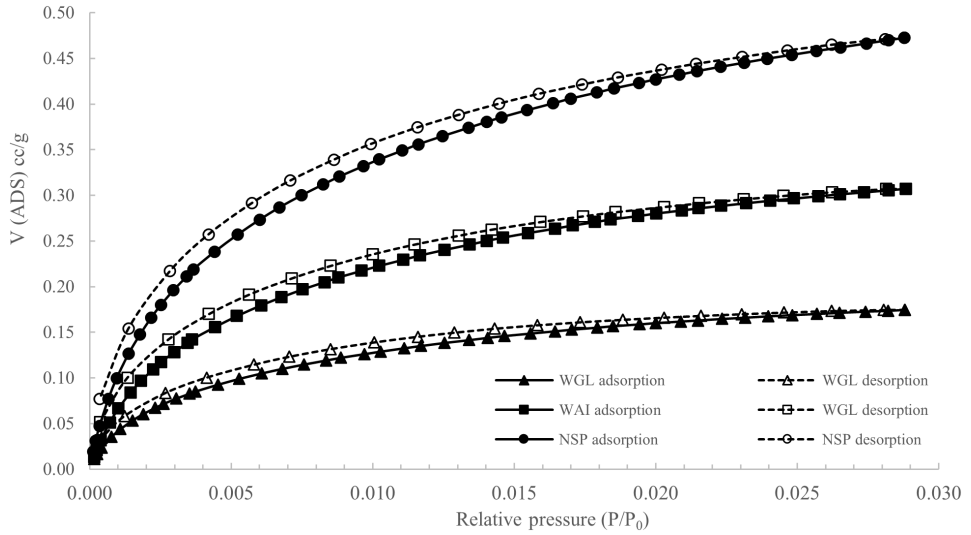

Figure 5. **N_2 adsorption and desorption isotherms of WAI, WGL and NSP biochars (P/P_0= Relative pressure, V (ADS) cc/g = Volume of adsorption cc/g).**

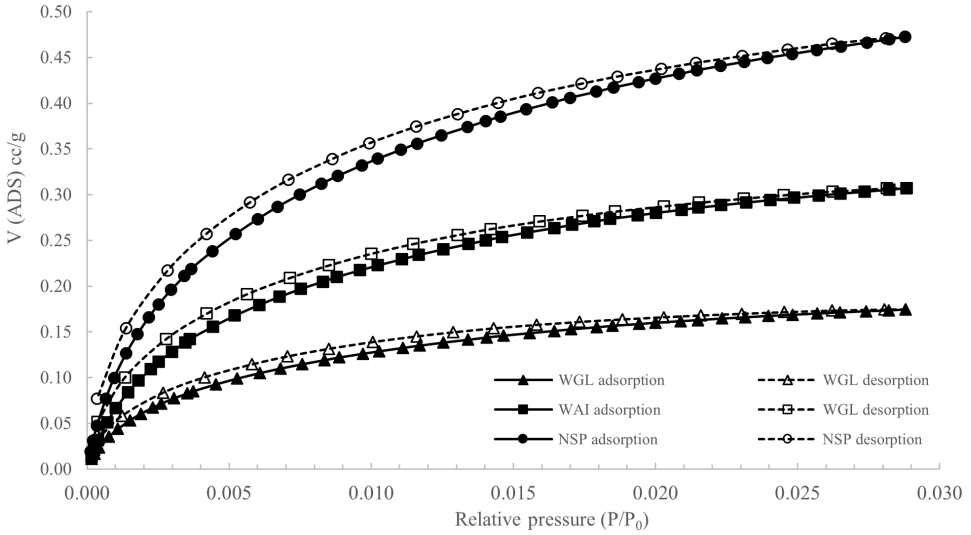

Figure 6. **CO_2 adsorption and desorption isotherms for WAI, WGL and NSP biochars (P/P_0= Relative pressure, V (ADS) cc/g = Volume of adsorption cc/g).**

distributions in this region (Figure 7b). In the mesoporous region, (16-150 Å), WGL biochar pore size distributions were much greater than both NSP and WGL biochar confirming WGL biochar has a more mesoporous structure (Figure 7a).

The values obtained demonstrate the complex pore network within the biochar, even though the surface area values are generally low compared to other biochars there is still a degree of both microporosity and mesoporosity within the biochars. Low surface area biochars may be unsuitable for use as soil amendments as the water holding capacity is relatively low and the low porosities are not conducive to promoting soil microbial growth (Ishii & Kadoya, 1994; Thies & Rillig, 2009), which play an important role in nutrient cycling (Lambers *et al.*, 2008). The surface area could be increased by increasing the pyrolysis temperature (Song & Guo, 2012; Tomczyk *et al.*, 2020). The fast pyrolysis of municipal sludge biochar at temperatures 500 - 900 °C showed that increasing temperatures resulted in a greater microporous network within the biochar (Chen *et al.*, 2014). Previous work has shown that the greatest enhancement of sewage sludge biochar porosity occurred between 400 - 600°C (Bagreev *et al.*, 2001). However heavy metal concentration in biochars generally increase with pyrolytic temperature (Lu *et al.*, 2013). This is because heavy metals

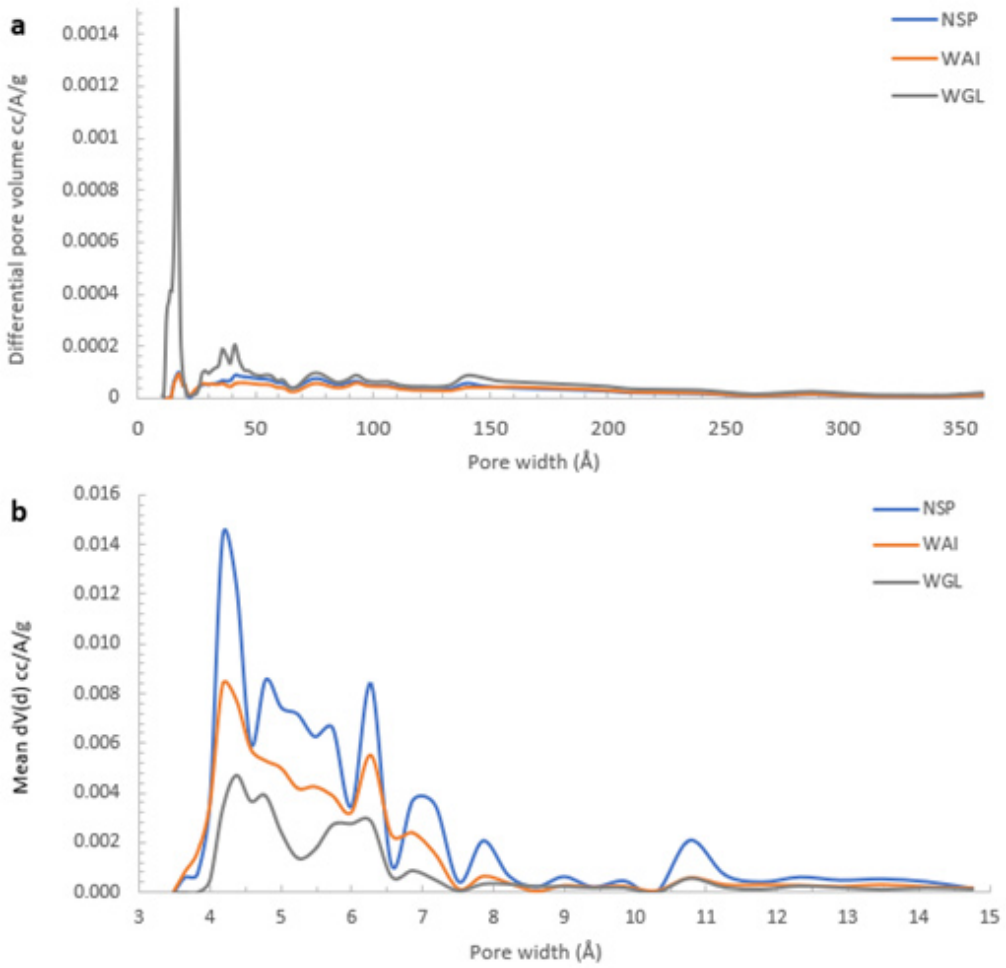

Figure 7. Pore volume weighted pore size-distribution derived from **a**) N_2 (mesopore region 2-50nm) and **b**) CO_2 (micropore region<2nm) for NSP, WAI and WGL biochars.

do not volatilize, so their concentration within the biochar increases with pyrolysis temperature (Chanaka Udayanga *et al.*, 2019; Hossain *et al.*, 2011; Wang *et al.*, 2021).

Zeta potential

Zeta (electrokinetic) potential signifies the net charge between the surface plane and slip plane of a colloidal particle (Hiemenz & Rajagopalan, 1997). Zeta potential values yield information about the external surface charges of biochar particles in solution and indicates the sorption and nutrient holding characteristics of the biochar in soil. Negatively charged surfaces are unlikely to sorb negatively charged ions such as phosphate but are more likely to sorb positive cations such as heavy metal ions and ammonium ions.

The zeta potential values for all three biochar samples were negative in the pH range 5.0-9.5, revealing that negative charges are carried on the surface of the biochar particles (Figure 8). FTIR spectra revealed the existence of oxygen containing functional groups ($–COO^-$ and–OH) on the biochars surface which can contribute considerably to surface charge of the biochars. The negative zeta potentials of all three biochars in the pH range 5.0 – 9.5 support this interpretation.

At acidic pH, the zeta potentials of the biochar samples became less negative, indicating that the association of $–COO^-$ and $–O^-$ with H^+ reduced the negative charge of the biochars. With increasing pH, the zeta potential of WAI_BC and NSP_BC biochars become more negative due to increasing deprotonation of the biochar surface functional groups (Yuan *et al.*, 2011). However, at pH above 7 there was an increase in zeta potential for WGL_BC from -23.4mV to -7.7mV indicating a decrease in negative surface charge. WGL_BC contains the highest ash content of all the biochars (Table 1), and it is likely this that contributes to the increase in zeta potential values at pH>7. The mechanism by which surface charge increases at high pH values cannot be explained by deprotonation of the surface functional groups in the case of WGL_BC. The higher ash content indicates some other mechanism occurring. Zeta potential of fine coal tailings containing several ash-forming

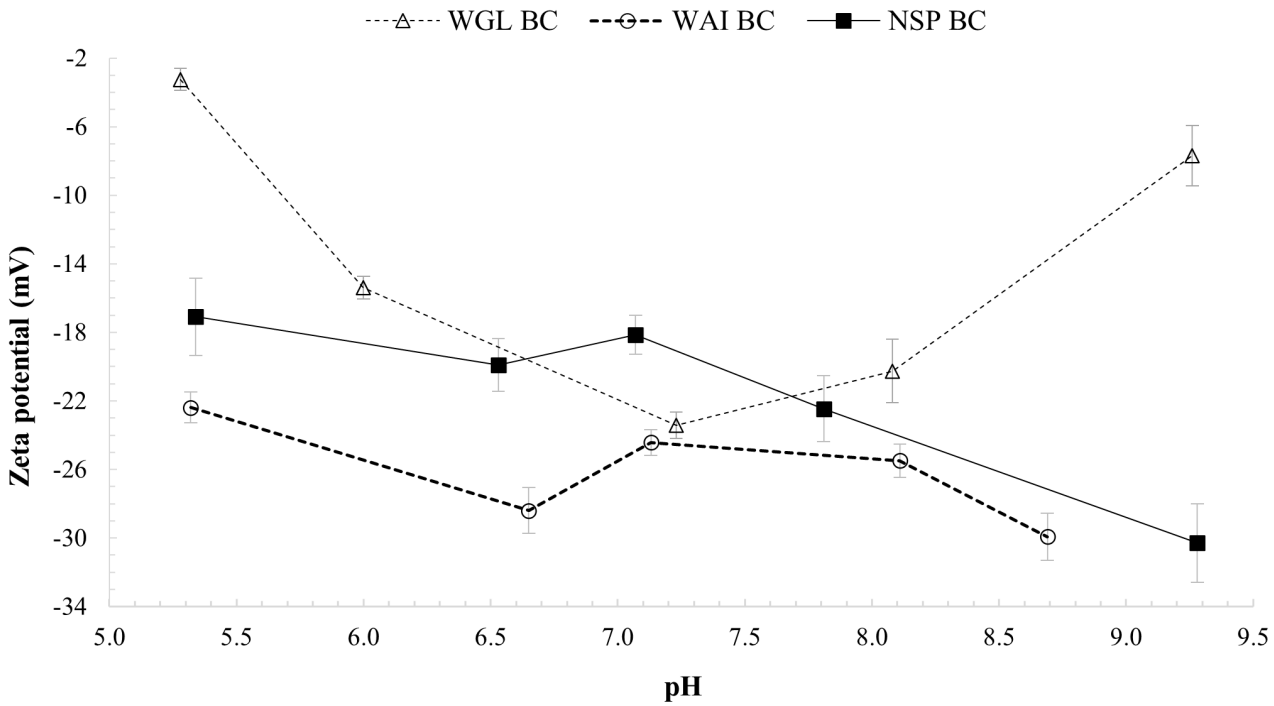

Figure 8. Zeta potentials of WGL_BC, WAI_BC and NSP_BC at pH values from 5-9.5.

minerals showed a similar trend which the authors attributed to the presence of alumina and silicate particles, which result in lower negative zeta potential values. They also noted that varying zeta potential values at high pH could be attributed to the binding of more cations such as Ca^{2+} (Kumar *et al.*, 2014). Positively charged calcium monohydroxide ions on the biochar surface would to some degree neutralize the negative surface charges resulting in less negative zeta potential values. (Liu *et al.*, 2002). It is possible that at pH values >9 WGL_BC would have positive zeta potential values and thus more likely to sorb negatively charged ions such as nitrate or phosphate.

X-ray diffraction (XRD)

X-ray diffraction (XRD) analysis of the biochars revealed that mineral components in the crystal form were present in all three biochars (Figure 9). Quartz was identified as the predominant crystalline phase with the highest peak at 2θ around 26.6° (d = 3.33 Å) in NSP and WGL biochars. WAI biochar exhibited a more intense peak relating to $CaSO_4$ (Anhydrite). Quartz, sylvite, calcite, calcium sulphate, albite were the most common phases identified. These minerals are formed during pyrolysis due to a reaction between CO_2 and alkaline-earth metals and alkaline oxyhydroxides.

Previous research has shown sewage sludge biochar to have a turbostratic structure where the carbon fraction is dominated by disordered graphitic crystallites (Srinivasan *et al.*, 2015; Uchimiya *et al.*, 2011). This is in discordance with the XRD results for NSP_BC and WGL_BC showing a distinct lack of C (002) diffraction peaks (2θ = 15-30°) and C (101) diffraction peaks (2θ = 40-50°) due to amorphous carbon structures and graphite structures respectively. However, WAI_BC showed a possible tail end of a diffraction peak (2θ = 15-30°) indicating an amorphous carbon structure (Figure 9). This peak is clearer for WAI_BC due to the lower -intensity quartz peaks present. The biochars studied here do have a very high ash content and the lack of these peaks for WGL_BC and NSP_BC is as a result of interference of high-intensity quartz peaks. Studies have shown that the high content of minerals, specifically quartz can affect the structural characterization of biochar carbon fraction (Feng *et al.*, 2015).

The difference in mineral composition between the three biochars could be due to possible contamination of FS by sand and grit caused by poorly lined containment structures (Niwagaba *et al.*, 2014). The containment structures at each location would have to be investigated to reach a definitive conclusion. The high content of nutrients within the biochars Ca, Si, and K and high alkalizing capacity of calcite ($CaCO_3$) indicate their potential use as a soil amendment particularly within low nutrient and acidic soils. Other carbonate minerals such as Thermonatrite and ankerite were also present. The high silicon content could also enhance biochar's role as soil amendment due to the significant influence of silicon in alleviating plant environmental stress (Chen *et al.*, 2011). Overall, the mineralogical composition of the biochars is in agreement with their high ash contents.

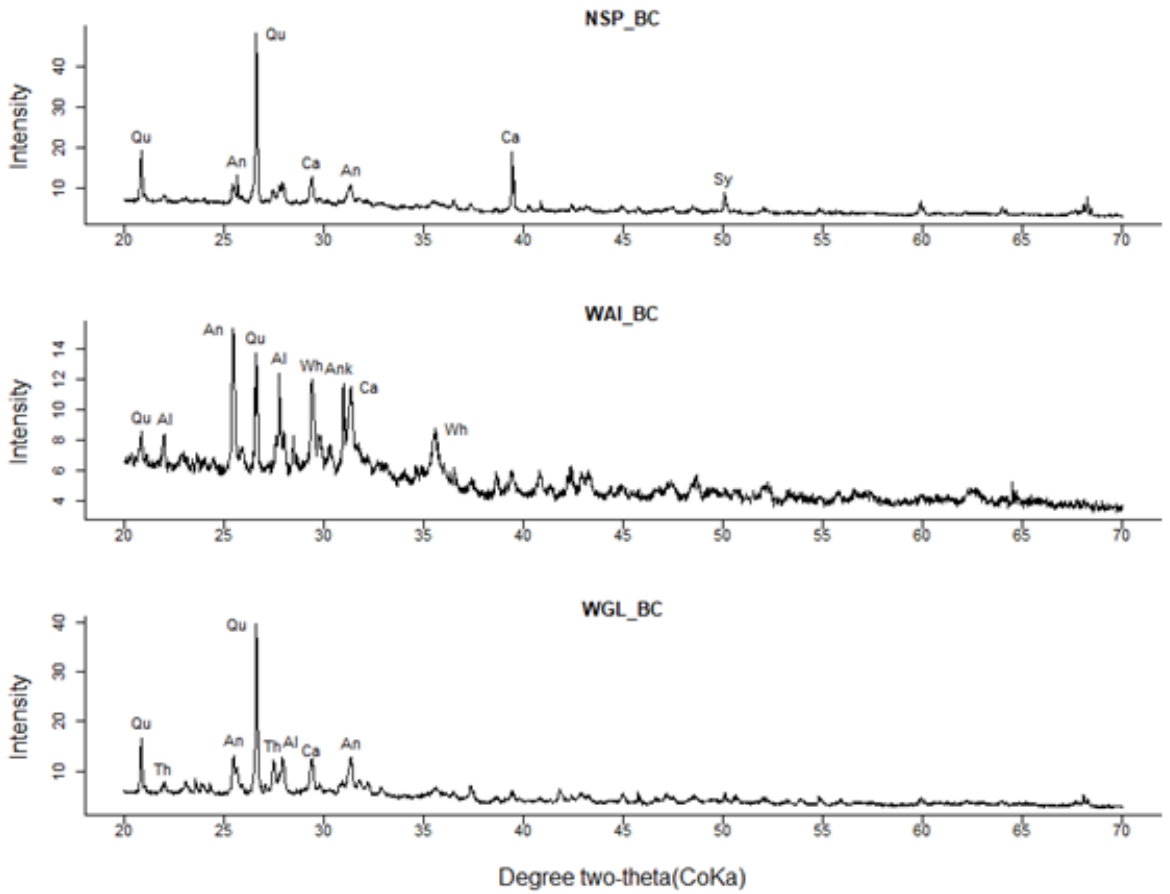

Figure 9. XRD patterns of NSP, WAI and WGL biochar (Qu= Quartz, Al=Albite, Ca=Calcite, An = Anhydrite, Sy = Sylvite, Wh = Whewellite, Ank=Ankerite, Th= Thermonatrite).

Scanning electron microscopy (SEM) with energy dispersive x-ray analysis (EDX)

SEM analysis reveals a complex porous structure evident in all biochars (Figure 10). The porous structure of biochars strongly resembles the cellular structure of the original feedstock (Fuertes *et al.*, 2010; Yao *et al.*, 2011). In the case of faecal sludge, cellular macroporous structures arise from undigested fibrous vegetable matter. The morphology of the biochar is honeycomb-like with cylindrical and slit like holes clearly observable. This porous structure can provide a specialized environment for the colonization of microbes (Thies & Rillig, 2012). This increase in mycorrhizal fungi contributes to increased mineralization of recalcitrant soil organic matter, ultimately improving soil and plant health (Anderson *et al.*, 2011; Zimmerman *et al.*, 2011). SEM images also show all three biochars have high ash content with EDX confirming the presence of mineral elements (Figure 11). The SEM images clearly showed a high presence of clay mineral particles/ash (white/grey) with a smaller amount of biochar particles present (black).

Visually WGL biochar had a higher ash content which is concurrent with the ash percentage from proximate analyses. EDX results on the biochar particles themselves revealed high volumes of carbon and oxygen (Figure 11). Also present were silicon, calcium aluminium, potassium, magnesium, phosphorus, and sodium all of which are beneficial to plant health.

Cation exchange capacity

Cation exchange capacity (CEC) enables biochars to adsorb cationic nutrients such as NH_4^+, Ca^{2+}, and K^+. It is thought this characteristic of biochar results predominantly from formation of carboxylic functional groups during oxidation (Cheng *et al.*, 2006).

There was a large variation in CEC values with WGL biochar (WGL BC) the highest CEC at 129.3 $cmolKg^{-1}$ and NSP biochar the lowest CEC at 41.9 $cmolKg^{-1}$ (Table 1). Fresh biochars from lignocellulosic biomass generally have lower CEC, with manure-based biochars exhibiting higher CEC values (Tag *et al.*, 2016). In the literature CEC values for biochar are highly variable, commonly ranging from 6 $cmol_{(+)}$ Kg^{-1} (Munera-Echeverri *et al.*, 2018) to 36.3 $cmol_{(+)}$ Kg^{-1} (Song & Guo, 2012) to as high as 304 $cmol_{(+)}$ Kg^{-1}.

Yuan *et al.* (2011) proposed that high ash content biomass creates high CEC biochars and that K, Na, Ca, Mg, and P in the feedstock would promote formation of O-containing acidic functional groups such as carboxylic, and phenolic groups on

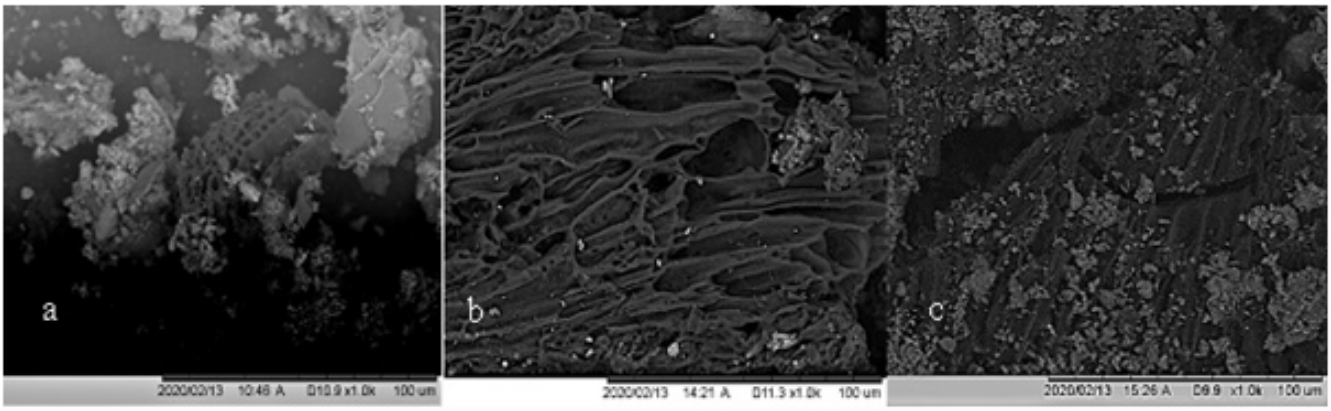

Figure 10. SEM micrograph of (**a**) Original WGL biochar, (**b**) Original NSP biochar, (**c**) Original WAI biochar.

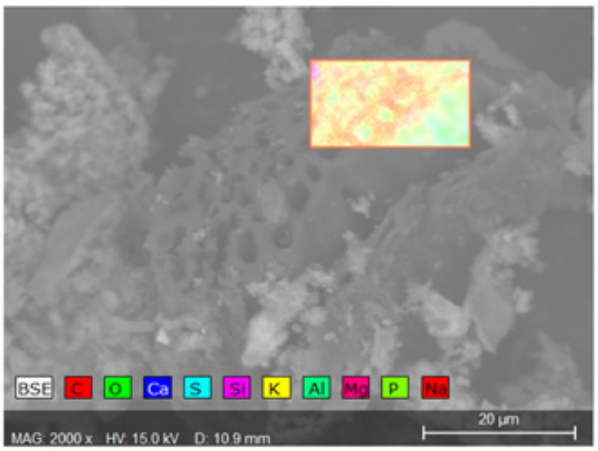

Element	Wt. %
C	70.55
O	21.00
Ca	3.24
S	1.62
Si	1.29
K	0.73
Al	0.63
Mg	0.50
P	0.27
Na	0.17

Figure 11. SEM-EDX map for all elements distribution across the area highlighted in image and associated energy dispersive X-ray (EDX) quantification of biochar.

biochar surface during pyrolysis and thus, result in higher CEC (Gaskin *et al.*, 2008). However, FTIR analysis showed a lack of acidic functional groups such as phenolic groups in these biochars. It is possible that the high ash content of these biochars could contribute to methodological problems in determining CEC (Graber *et al.*, 2017). There is a large range of CEC values reported in the literature and measurements are often poorly reproducible (Munera-Echeverri *et al.*, 2018). FTIR shows that there are carbonates and silicates present in these biochars which would result in the release of base cations and interference with the sum of measured exchangeable base cations (Munera-Echeverri *et al.*, 2018). WGL biochar records the highest CEC value (129.3 ± 2.3 $cmol.kg^{-1}$) and the highest ash content of all three biochars implying that it is the high ash content that is responsible for the high CEC value.

Conclusion

Overall, all three faecal sludge biochars had a high ash content, high pH, low carbon content, negative surface charge and low specific surface areas and pore volumes. The similarity of FTIR spectra between biochars signifies a uniformity of the organic component of all three biochars. Warangal biochar had a significantly higher ash content and pH compared to the Narsapur and Wai biochar. There were also differences in XRD spectra between biochars. These differences are likely related to the contamination of faecal sludge in the containment structure by sand or grit, or the sintered mineral deposits in the reactor itself. The variability of these faecal sludge biochar properties highlights the differences between small-scall laboratory and full-scale "real world" biochar production. Control over every single variable in large-scale faecal sludge biochar production is difficult and routine inspections of every containment structure at every location would be time-consuming. However, the pH and ash content of the biochars could be monitored periodically at the treatment plant. Overall, the properties of these biochars, in particular the high alkalinity, shows their potential use as soil amendments. Future work should determine the biochars total and plant available macro-and

micronutrient concentrations. Further investigation into the evaluation of these biochars as soil amendments with a focus on application to acidic soils is also recommended.

Data availability

Underlying data

Mendeley Data: FS biochar properties. https://doi.org/10.17632/2xsdbdb38k.3 (Nicholas, 2022)

This project contains the following files:

- Figure 2 FTIR original_final600.tiff- FTIR spectra unamended biochars
- Figure 3 FTIR ashed_final600.tiff – FTIR spectra of ashed biochars
- Figure 4 FTIR acidwashed_final600.tiff – FTIR spectra of acid washed biochars
- Figure 5 Nitrogen.tif – N_2 adsorption and desorption isotherms of WAI, WGL and NSP biochars
- Figure 6 CO2.tif – CO_2 adsorption and desorption isotherms of WAI, WGL and NSP biochars
- Figure 7 pore volumes600.tif - Pore volume weighted pore size-distribution graphs for a) N_2 (mesopore region 2-50nm) and b) CO_2 (micropore region<2nm) for NSP, WAI and WGL biochars.
- Figure 8 zeta potential600.tif – Zeta potentials of WGL_BC, WAI_BC and NSP_BC at pH values from 5-9.5
- Figure 9 XRD500.tif - XRD spectra of NSP, WAI and WGL biochar
- Figure 10 SEM500.tif- SEM biochar images
- Figure 11 EDX500.tif – EDX biochar image
- CEC2.xlsx – All cation exchange capacity data
- CHNS_results.xlsx – Elemental analysis (CHNS) data
- FTIR Data2.xlsx – all FTIR data
- XRD15.xlsx – Xray diffraction data
- N2 isotherm data.xlsx – Nitrogen adsorption and desorption isotherms data
- N2 Pore volume BET data.xlsx – Nitrogen pore volume data
- CO2 isotherm data.xlsx – Carbon dioxide adsorption and desorption isotherms data
- CO2 BET pore volume data.xlsx – Carbon dioxide pore volume data
- ph and electrical conductivity raw data.xlsx – pH and electrical conductivity raw data
- Raw zeta potential data.xlsx – raw zeta potential data

CRediT authorship contribution statement

Larissa Nicholas: Conceptualization, Methodology, Investigation, Writing – original draft, Project Administration, Visualization. Ian Mabbett: Conceptualization, Methodology, Writing – review and editing, Funding Acquisition, Supervision. Henry Apsey: Investigation. Iain Robertson: Writing – review & editing.

Acknowledgements

The authors thank the staff of Tide Technocrats Ltd. for the supply of biochar, Tom Dunlop (Swansea University), Mariolino Carta (Swansea University), Gabriel Sigmund (University of Vienna) and Maria Santiso Taboada (University of Santiago de Compostela). XRD and SEM analysis assistance provided by Swansea University College of Engineering AIM facility, which is funded in part by the EPSRC (EP/M028267/1), the European Regional Development Fund through the Welsh Government (80708) and Ser Solar project via Welsh Government.

References

Agrafioti E, Bouras G, Kalderis D, *et al.*: **Biochar production by sewage sludge pyrolysis.** *J Anal Appl Pyrolysis.* 2013; **101**: 72–78.
Publisher Full Text

Anderson CR, Condron LM, Clough TJ, *et al.*: **Biochar induced soil microbial community change: Implications for biogeochemical cycling of carbon, nitrogen and phosphorus.** *Pedobiologia (Jena).* 2011; **54**(5–6): 309–320.
Publisher Full Text

Andriessen N, Ward BJ, Strande L: **To char or not to char? Review of technologies to produce solid fuels for resource recovery from faecal sludge.** *J Water Sanit Hyg Dev.* 2019; **9**(2): 210–224.
Publisher Full Text

ASTM D 1762-84: **Standard Test Method for Chemical Analysis of Wood Charcoal.** *ASTM Int.* 2011; **84**: 1–2.
Publisher Full Text

Bagreev A, Bandosz TJ, Locke DC: **Pore structure and surface chemistry of adsorbents obtained by pyrolysis of sewage sludge-derived fertilizer.** *Carbon NY.* 2001; **39**(13): 1971–1979.
Publisher Full Text

Banik C, Lawrinenko M, Bakshi S, *et al.*: **Impact of Pyrolysis Temperature and Feedstock on Surface Charge and Functional Group Chemistry of Biochars.** *J Environ Qual.* 2018; **47**(3): 452–461.
PubMed Abstract | Publisher Full Text

Bleuler M, Gold M, Strande L, *et al.*: **Pyrolysis of Dry Toilet Substrate as a Means of Nutrient Recycling in Agricultural Systems: Potential Risks and Benefits.** *Waste Biomass Valor.* 2021; **12**: 4171–4183.
Publisher Full Text

Brunauer S, Emmett PH, Teller E: **Adsorption of Gases in Multimolecular Layers.** *J Am Chem Soc.* 1938; **60**(2): 309–319.
Publisher Full Text

Calderón FJ, McCarty GW, Reeves JB: **Pyrolisis-MS and FT-IR analysis of fresh and decomposed dairy manure.** *J Anal Appl Pyrolysis.* 2006; **76**(1–2): 14–23.
Publisher Full Text

Castan S, Sigmund G, Hüffer T, *et al.*: **Biochar particle aggregation in soil pore water: The influence of ionic strength and interactions with pyrene.** *Environ Sci Process Impacts.* 2019; **21**(10): 1722–1728.
PubMed Abstract | Publisher Full Text

Chan KY, Van Zwieten L, Meszaros I, *et al.*: **Agronomic values of greenwaste biochar as a soil amendment.** *Aust J Soil Res.* 2007; **45**(8): 629–634.
Publisher Full Text

Chanaka Udayanga WD, Veksha A, Giannis A, *et al.*: **Insights into the speciation of heavy metals during pyrolysis of industrial sludge.** *Sci Total Environ.* 2019; **691**: 232–242.
PubMed Abstract | Publisher Full Text

Chen B, Zhou D, Zhu L: **Transitional adsorption and partition of nonpolar and polar aromatic contaminants by biochars of pine needles with different pyrolytic temperatures.** *Environ Sci Technol.* 2008; **42**(14): 5137–5143.
PubMed Abstract | Publisher Full Text

Chen T, Zhang Y, Wang H, *et al.*: **Influence of pyrolysis temperature on characteristics and heavy metal adsorptive performance of biochar derived from municipal sewage sludge.** *Bioresour Technol.* 2014; **164**: 47–54.
PubMed Abstract | Publisher Full Text

Chen W, Yao X, Cai K, *et al.*: **Silicon alleviates drought stress of rice plants by improving plant water status, photosynthesis and mineral nutrient absorption.** *Biol Trace Elem Res.* 2011; **142**(1): 67–76.
PubMed Abstract | Publisher Full Text

Cheng CH, Lehmann J, Thies JE, *et al.*: **Oxidation of black carbon by biotic and abiotic processes.** *Org Geochem.* 2006; **37**(11): 1477–1488.
Publisher Full Text

Claoston N, Samsuri AW, Ahmad Husni MH, *et al.*: **Effects of pyrolysis temperature on the physicochemical properties of empty fruit bunch and rice husk biochars.** *Waste Manag Res.* 2014; **32**(4): 331–339.
PubMed Abstract | Publisher Full Text

Coates J: **Encyclopedia of Analytical Chemistry -Interpretation of Infrared Spectra, A Practical Approach.** *Encycl Anal Chem.* 2004; 1–23.

Crombie K, Mašek O, Cross A, *et al.*: **Biochar - synergies and trade-offs between soil enhancing properties and C sequestration potential.** *GCB Bioenergy.* 2015; **7**(5): 1161–1175.
Publisher Full Text

Crombie K, Mašek O, Sohi SP, *et al.*: **The effect of pyrolysis conditions on biochar stability as determined by three methods.** *GCB Bioenergy.* 2013; **5**(2): 122–131.
Publisher Full Text

Davis WM, Erickson CL, Johnston CT, *et al.*: **Quantitative Fourier Transform Infrared spectroscopic investigation humic substance functional group composition.** *Chemosphere.* 1999; **38**(12): 2913–2928.
Publisher Full Text

Deacon GB, Phillips RJ: **Relationships between the carbon-oxygen stretching frequencies of carboxylato complexes and the type of carboxylate coordination.** *Coord Chem Rev.* 1980; **33**(3): 227–250.
Publisher Full Text

Downs RT, Hall-Wallace M: **The American Mineralogist crystal structure database.** *Am Mineral.* 2003; **88**: 247–250.
Publisher Full Text

EEC: **91/692/EEC Council Directive of 12 June 1986 on the Protection of the Environment, and in Particular of the Soil, when Sewage Sludge Is Used in Agriculture**. EEC. 1986.

Ellerbrock RH, Gerke HH: **FTIR spectral band shifts explained by OM-cation interactions.** *J Plant Nutr Soil Sci.* 2021; **184**(3): 388–397.
Publisher Full Text

Enders A, Hanley K, Whitman T, *et al.*: **Characterization of biochars to evaluate recalcitrance and agronomic performance.** *Bioresour Technol.* 2012; **114**: 644–653.
PubMed Abstract | Publisher Full Text

Enders A, Lehmann J: **Proximate analyses for characterising biochars.** *Biochar A Guid to Anal Methods.* 2015; 9–22.

European Biochar Foundation: **Guidelines for a Sustainable Production of Biochar.** *Eur Biochar Found.* 2016; 1–22.

Falaras P: **Cottonseed Oil Bleaching by Acid-Activated Montmorillonite.** *Clay Miner.* 1999; **34**(2): 221–232.
Publisher Full Text

Farmer VC: **Chapter 1 Vibrational Spectroscopy in Mineral Chemistry**. 1974; 1–10.
Publisher Full Text

Feng H, Zheng M, Dong H, *et al.*: **Three-dimensional honeycomb-like hierarchically structured carbon for high-performance supercapacitors derived from high-ash-content sewage sludge.** *J Mater Chem A.* 2015; **3**(29): 15225–15234.
Publisher Full Text

Fuertes AB, Arbestain MC, Sevilla M, *et al.*: **Chemical and structural properties of carbonaceous products obtained by pyrolysis and hydrothermal carbonisation of corn stover.** *Aust J Soil Res.* 2010; **48**(7): 618–626.
Publisher Full Text

Gaskin JW, Steiner C, Harris K, *et al.*: **Effect of Low-Temperature Pyrolysis Conditions on Biochar for Agricultural Use.** *Trans ASABE.* 2008; **51**(6): 2061–2069.
Publisher Full Text

Gaskin JW, Speir A, Morris LM, *et al.*: **Potential for Pyrolysis Char to Affect Soil Moisture and Nutrient Status of a Loamy Sand Soil**. 2007.
Reference Source

Glaser B, Haumaier L, Guggenberger G, *et al.*: **The 'Terra Preta' phenomenon: A model for sustainable agriculture in the humid tropics.** *Naturwissenschaften.* 2001; **88**(1): 37–41.
PubMed Abstract | Publisher Full Text

Gold M, Cunningham M, Bleuler M, *et al.*: **Operating parameters for three resource recovery options from slow-pyrolysis of faecal sludge.** *J Water Sanit Hyg Dev.* 2018; **8**(4): 707–717.
Publisher Full Text

Graber E, Singh B, Lehmann J, *et al.*: **Determination of Cation Exchange Capacity in Biochar**. In: Singh, B., Camps-Arbestain, M., Lehmann, J. (Eds.), *Biochar: A Guide to Analytical Methods*. Csiro Publishing, 2017; 74–84.

Gražulis S, Chateigner D, Downs RT, *et al.*: **Crystallography Open Database - An open-access collection of crystal structures.** *J Appl Crystallogr.* 2009; **42**(Pt 4): 726–729.
PubMed Abstract | Publisher Full Text | Free Full Text

Gražulis S, Daškevič A, Merkys A, *et al.*: **Crystallography Open Database (COD): An open-access collection of crystal structures and platform for world-wide collaboration.** *Nucleic Acids Res.* 2012; **40**(Database issue): 420–427.
PubMed Abstract | Publisher Full Text | Free Full Text

Gražulis S, Merkys A, Vaitkus A, *et al.*: **Computing stoichiometric molecular composition from crystal structures.** *J Appl Crystallogr.* 2015; **48**(Pt 1): 85–91.
PubMed Abstract | Publisher Full Text | Free Full Text

Gwenzi W, Munondo R: **Long-term impacts of pasture irrigation with treated sewage effluent on nutrient status of a sandy soil in Zimbabwe.** *Nutr Cycl Agroecosystems.* 2008; **82**: 197–207.
Publisher Full Text

Haller L, Hutton G, Bartram J: **Estimating the costs and health benefits of water and sanitation improvements at global level.** *J Water Health.* 2007; **5**(4): 467–480.
PubMed Abstract | Publisher Full Text

Hiemenz PC, Rajagopalan R: **Principles of Colloid and Surface Chemistry, Revised and Expanded**. 3rd ed. CRC Press. 1997.
Publisher Full Text

Hossain MK, Strezov V, Chan KY, *et al.*: **Influence of pyrolysis temperature on production and nutrient properties of wastewater sludge biochar.** *J Environ Manage.* 2011; **92**(1): 223–8.
PubMed Abstract | Publisher Full Text

Hutton G, Bartram J: **Global costs of attaining the Millennium Development Goal for water supply and sanitation.** *Bull World Health Organ.* 2008; **86**(1): 13–19.
PubMed Abstract | Publisher Full Text | Free Full Text

IBI: **Standardized Product Definition and Product Testing Guidelines for Biochar 7 That Is Used in Soil.** [WWW Document]. 2015; (accessed 11.10.20).
Reference Source

Ishii T, Kadoya K: **Effects of charcoal as a soil conditioner on citrus growth and vesicular-arbuscular mycorrhizal development.** *J Japanese Soc Hortic Sci.* 1994; **63**(3): 529–535.
Publisher Full Text

Jeffery S, Verheijen FGA, van der Velde M, *et al.*: **A quantitative review of the effects of biochar application to soils on crop productivity using meta-analysis.** *Agric Ecosyst Environ.* 2011; **144**(1): 175–187.
Publisher Full Text

Jiang W, Saxena A, Song B, *et al.*: **Elucidation of functional groups on gram-positive and gram-negative bacterial surfaces using infrared spectroscopy.** *Langmuir.* 2004; **20**(26): 11433–11442.
PubMed Abstract | Publisher Full Text

Keiluweit M, Nico PS, Johnson MG, *et al.*: **Dynamic molecular structure of plant biomass-derived black carbon (biochar).** *Environ Sci Technol.* 2010; **44**(4): 1247–1253.
PubMed Abstract | Publisher Full Text

Khan S, Chao C, Waqas M, *et al.*: **Sewage sludge biochar influence upon rice (*Oryza sativa L*) yield, metal bioaccumulation and greenhouse gas emissions from acidic paddy soil.** *Environ Sci Technol.* 2013; **47**(15): 8624–8632.
PubMed Abstract | Publisher Full Text

Kim P, Johnson A, Edmunds CW, *et al.*: **Surface functionality and carbon structures in lignocellulosic-derived biochars produced by fast pyrolysis.** *Energy and Fuels.* 2011; **25**(10): 4693–4703.
Publisher Full Text

Klasson KT, Lima IM, Boihem LL: **Poultry manure as raw material for mercury adsorbents in gas applications.** *J Appl Poult Res.* 2009; **18**(3): 562–569.
Publisher Full Text

Koetlisi KA, Muchaonyerwa P: **Biochar Types from Latrine Waste and Sewage Sludge Differ in Physico-Chemical Properties and Cadmium Adsorption.** *Am J Appl Sci.* 2017; **14**(11): 1039–1048.
Publisher Full Text

Kosek M, Bern C, Guerrant RL: **The global burden of diarrhoeal disease, as estimated from studies published between 1992 and 2000.** *Bull World Health Organ.* 2003; **81**(3): 197–204.
PubMed Abstract | Free Full Text

Krueger BC, Fowler GD, Templeton MR, *et al.*: **Resource recovery and biochar characteristics from full-scale faecal sludge treatment and co-treatment**

with agricultural waste. *Water Res.* 2020; **169**: 115253.
PubMed Abstract | Publisher Full Text | Free Full Text

Kumar S, Bhattacharya S, Mandre NR: **Characterization and flocculation studies of fine coal tailings.** *J South African Inst Min Metall.* 2014; **114**: 945–949.

Lambers H, Chapin FS, Pons TL: **Plant physiological ecology: Second edition.** *Plant Physiol Ecol Second Ed.* 2008; 1–604.
Publisher Full Text

Lehmann J, Joseph S: **Biochar for Environmental Management, Biochar for Environmental Management**. 2012.

Lima I, Klasson KT, Uchimiya M: **Selective release of inorganic constituents in broiler manure biochars under different post-activation treatments.** *J Residuals Sci Technol.* 2016; **13**(1): 37–48.
Reference Source

Liu J, Zhou Z, Xu Z: **Electrokinetic study of hexane droplets in surfactant solutions and process water of bitumen extraction systems.** *Ind Eng Chem Res.* 2002; **41**(1): 52–57.
Publisher Full Text

Liu X, Li Z, Zhang Y, *et al.*: **Characterization of human manure-derived biochar and energy-balance analysis of slow pyrolysis process.** *Waste Manag.* 2014; **34**(9): 1619–1626.
PubMed Abstract | Publisher Full Text

Lou L, Luo L, Wang L, *et al.*: **The influence of acid demineralization on surface characteristics of black carbon and its sorption for pentachlorophenol.** *J Colloid Interface Sci.* 2011; **361**(1): 226–231.
PubMed Abstract | Publisher Full Text

Lu H, Zhang W, Wang S, *et al.*: **Characterization of sewage sludge-derived biochars from different feedstocks and pyrolysis temperatures.** *J Anal Appl Pyrolysis.* 2013; **102**: 137–143.
Publisher Full Text

Mara D, Lane J, Scott B, *et al.*: **Sanitation and health.** *PLoS Med.* 2010; **7**(11): e1000363.
PubMed Abstract | Publisher Full Text | Free Full Text

Merkys A, Vaitkus A, Butkus J, *et al.*: ***COD::CIF::Parser*: An error-correcting CIF parser for the Perl language.** *J Appl Crystallogr.* 2016; **49**(Pt 1): 292–301.
PubMed Abstract | Publisher Full Text | Free Full Text

Mokaya R, Jones W: **Pillared clays and pillared acid-activated clays: A comparative-study of physical, acidic, and catalytic properties.** *J Catal.* 1995; **153**(1): 76–85.
Publisher Full Text

Munera-Echeverri JL, Martinsen V, Strand LT, *et al.*: **Cation exchange capacity of biochar: An urgent method modification.** *Sci Total Environ.* 2018; **642**: 190–197.
PubMed Abstract | Publisher Full Text

Nicholas H: **"FS biochar properties"**. Mendeley Data, V3 [Dataset]. 2022.
http://www.doi.org/10.17632/2xsdbdb38k.3

Niwagaba CB, Mbéguéré M, Strande L: **Faecal sludge quantification, characterisation and treatment objectives.** In: Linda Strande, Mariska Ronteltap, D.B. (Editor) (Ed.), *Faecal Sludge Management: Systems Approach for Implementation and Operation.* IWA Publishing, London, UK, 2014; 19–44.
Reference Source

Novak JM, Busscher WJ, Laird DL, *et al.*: **Impact of biochar amendment on fertility of a southeastern coastal plain soil.** *Soil Sci.* 2009; **174**: 105–112.
Publisher Full Text

Peech M, Alexander LT, Dean LA, *et al.*: **Methods of Soil Analysis for Soil Fertility Investigations.** Washington, DC, 1947.
Reference Source

Qian L, Chen B: **Dual role of biochars as adsorbents for aluminum: The effects of oxygen-containing organic components and the scattering of silicate particles.** *Environ Sci Technol.* 2013; **47**: 8759–8768.
PubMed Abstract | Publisher Full Text

Quirós M, Gražulis S, Girdzijauskaitė S, *et al.*: **Using SMILES strings for the description of chemical connectivity in the Crystallography Open Database.** *J Cheminform.* 2018; **10**(1): 23.
PubMed Abstract | Publisher Full Text | Free Full Text

Rehrah D, Reddy MR, Novak JM, *et al.*: **Production and characterization of biochars from agricultural by-products for use in soil quality enhancement.** *J Anal Appl Pyrolysis.* 2014; **108**: 301–309.
Publisher Full Text

Samsuri AW, Sadegh-Zadeh F, Seh-Bardan BJ: **Adsorption of As(III) and As(V) by Fe coated biochars and biochars produced from empty fruit bunch and rice husk.** *J Environ Chem Eng.* 2013; **1**(4): 981–988.
Publisher Full Text

Schimmelpfennig S, Glaser B: **One Step Forward toward Characterization: Some Important Material Properties to Distinguish Biochars.** *J Environ Qual.* 2012; **41**: 1001–1013.
Publisher Full Text

Shahrokh Abadi MH, Delbari A, Fakoor Z, *et al.*: **Effects of annealing temperature on infrared spectra of SiO_2 extracted from rice husk.** *J Ceram Sci Technol.* 2015; **6**: 41–45.
Publisher Full Text

Sharma RK, Wooten JB, Baliga VL, *et al.*: **Characterization of chars from pyrolysis of lignin.** *Fuel.* 2004; **83**: 1469–1482.
Publisher Full Text

Sing KSW, Williams RT: **Physisorption hysteresis loops and the characterization of nanoporous materials.** *Adsorpt Sci Technol.* 2004; **22**: 773–782.
Publisher Full Text

Singh B, Dolk MM, Shen Q, *et al.*: **Biochar pH, electrical conductivity and liming potential.** *Biochar A Guid to Anal Methods.* 2017; 23–38.
Reference Source

Singh B, Singh BP, Cowie AL: **Characterisation and evaluation of biochars for their application as a soil amendment.** *Aust J Soil Res.* 2010; **48**: 516–525.
Publisher Full Text

Smider B, Singh B: **Agronomic performance of a high ash biochar in two contrasting soils.** *Agric Ecosyst Environ.* 2014; **191**: 99–107.
Publisher Full Text

Socrates G: **Infrared and Raman Characteristic Group Frequencies, 3rd ed.** John Wiley & Sons, Hoboken, NJ. 2001.
Reference Source

Song W, Guo M: **Quality variations of poultry litter biochar generated at different pyrolysis temperatures.** *J Anal Appl Pyrolysis.* 2012; **94**: 138–145.
Publisher Full Text

Srinivasan P, Sarmah AK, Smernik R, *et al.*: **A feasibility study of agricultural and sewage biomass as biochar, bioenergy and biocomposite feedstock: Production, characterization and potential applications.** *Sci Total Environ.* 2015; **512–513**: 495–505.
PubMed Abstract | Publisher Full Text

Strande L, Brdjanovic D, Ronteltap M: **Faecal Sludge Management: Systems Approach for Implementation and Operation**. IWA Publishing, London, UK. 2014.
Publisher Full Text

Stuart BH: **Infrared Spectroscopy: Fundamentals and Applications, Analytical Techniques in the Sciences**. John Wiley & Sons, Ltd, Chichester, UK. 2004.
Publisher Full Text

Tag AT, Duman G, Ucar S, *et al.*: **Effects of feedstock type and pyrolysis temperature on potential applications of biochar.** *J Anal Appl Pyrolysis.* 2016; **120**: 200–206.
Publisher Full Text

Thies JE, Rillig MC: **Characteristics of biochar: biological properties**. in: Lehmann, J., Joseph, S. (Eds.), *Biochar for Environmental Management*. Earthscan, Gateshead, UK, 2009; 85–105.
Publisher Full Text

Thies JE, Rillig MC: **Characteristics of biochar: Biological properties.** *Biochar Environ Manag Sci Technol.* 2012; 85–105.

Thomas Klasson K, Uchimiya M, Lima IM: **Uncovering surface area and micropores in almond shell biochars by rainwater wash.** *Chemosphere.* 2014; **111**: 129–134.
PubMed Abstract | Publisher Full Text

Thommes M, Kaneko K, Neimark AV, *et al.*: **Physisorption of gases, with special reference to the evaluation of surface area and pore size distribution (IUPAC Technical Report).** *Pure Appl Chem.* 2015; **87**: 1051–1069.
Publisher Full Text

Tide Technocrats: **Thermal FSSTP [WWW Document]**. n.d; (accessed 7.8.22).
Reference Source

Tomczyk A, Sokołowska Z, Boguta P: **Biochar physicochemical properties: pyrolysis temperature and feedstock kind effects.** *Rev Environ Sci Biotechnol.* 2020; **19**: 191–215.
Publisher Full Text

Uchimiya M, Wartelle LH, Klasson KT, *et al.*: **Influence of pyrolysis temperature on biochar property and function as a heavy metal sorbent in soil.** *J Agric Food Chem.* 2011; **59**(6): 2501–2510.
PubMed Abstract | Publisher Full Text

UN: **Transforming our world: the 2030 Agenda for Sustainable Development**. United Nations, New York [WWW Document]. 2015; (accessed 1.13.22).
Reference Source

UNICEF, WHO: **Progress on Drinking Water, Sanitation and Hygiene**. Joint Monitoring Programme 2017 Update and SDG Baselines. Who 2017; 66.
Reference Source

UNICEF/WHO: **Progress on Household Drinking Water**. 2021.

von Uexküll H, Mutert E: **Global extent, development and economic impact of acid soils.** In: *Plant–Soil Interactions at Low PH: Principles and Management*. Kluwer Academic Publishers, Dordrecht, The Netherlands, 1995; 5–19.
Publisher Full Text

Wang Z, Liu S, Liu K, *et al.*: **Effect of temperature on pyrolysis of sewage sludge: Biochar properties and environmental risks from heavy metals.** *E3S Web Conf.* 2021; **237**.

Weber K, Quicker P: **Properties of biochar.** *Fuel.* 2018; **217**: 240–261.
Publisher Full Text

Wen B, Zhang JJ, Zhang SZ, *et al.*: **Phenanthrene sorption to soil humic acid and different humin fractions.** *Environ Sci Technol.* 2007; **41**(9): 3165–3171.
PubMed Abstract | Publisher Full Text

WHO, UNICEF: **Progress on household drinking water, sanitation and hygiene 2000-2017. Special focus on inequalities**. New York: United Nations Children's Fund (UNICEF) and World Health Organization, 2017; 2019.
Reference Source

Woldetsadik D, Drechsel P, Marschner B, *et al.*: **Effect of biochar derived from**

faecal matter on yield and nutrient content of lettuce (*Lactuca sativa*) in two contrasting soils. *Environ Syst Res.* 2018; **6**.
Publisher Full Text

Yao Y, Gao B, Inyang M, *et al.*: **Biochar derived from anaerobically digested sugar beet tailings: Characterization and phosphate removal potential.** *Bioresour Technol.* 2011; **102**(10): 6273–6278.
PubMed Abstract | Publisher Full Text

Yuan JH, Xu RK, Zhang H: **The forms of alkalis in the biochar produced from crop residues at different temperatures.** *Bioresour Technol.* 2011; **102**(3): 3488–3497.
PubMed Abstract | Publisher Full Text

Zhang J, Lü F, Zhang H, *et al.*: **Multiscale visualization of the structural and characteristic changes of sewage sludge biochar oriented towards potential agronomic and environmental implication.** *Sci Rep.* 2015; **5**: 9406.
PubMed Abstract | Publisher Full Text | Free Full Text

Zhao L, Cao X, Mašek O, *et al.*: **Heterogeneity of biochar properties as a function of feedstock sources and production temperatures.** *J Hazard Mater.* 2013; **256–257**: 1–9.
PubMed Abstract | Publisher Full Text

Zielińska A, Oleszczuk P, Charmas B, *et al.*: **Effect of sewage sludge properties on the biochar characteristic.** *J Anal Appl Pyrolysis.* 2015; **112**: 201–213.
Publisher Full Text

Zimmerman AR, Gao B, Ahn MY: **Positive and negative carbon mineralization priming effects among a variety of biochar-amended soils.** *Soil Biol Biochem.* 2011; **43**(6): 1169–1179.
Publisher Full Text